Nuclear Materials and Energy 3–4 (2015) 12–16

Contents lists available at ScienceDirect

Nuclear Materials and Energy

journal homepage: www.elsevier.com/locate/nme

The dissolution of helium in La-doped UO_2 as a surrogate of hypo-stoichiometric UO_2

Z. Talip *, T. Wiss, A. Janssen, J.-Y. Colle, J. Somers, R.J.M. Konings

European Commission, Joint Research Centre, Institute for Transuranium Elements, P. O. Box 2340, 76125 Karlsruhe, Germany

ARTICLE INFO

Article history:
Received 14 December 2014
Accepted 27 January 2015
Available online 10 June 2015

Keywords:
Helium
Diffusion
Hypo-stoichiometric UO_2

ABSTRACT

In this work, the dissolution of helium in La-doped UO_2 samples was studied by helium infusion in an autoclave followed by thermal desorption (laser heating) coupled to mass spectrometer systems for the determination of helium release rate and the total helium quantity. Lanthanum was chosen as a dopant in UO_2 to study the effect of hypo-stoichiometry on helium solubility together with the impurity effect. Comparison of the dissolved He quantity from the samples with different La content showed that the dissolved He quantity slightly increases with increasing oxygen vacancy concentration in the samples.

1. Introduction

Formation of a large quantity of helium by α-decay is one of the main consequences arising from the presence of actinides in nuclear fuel [1,2]. Due to its low solubility [3–8], helium can precipitate in the spent fuel matrix and induce swelling which in turn could affect the mechanical properties of the spent fuel during long-term storage and final disposal [9]. Theoretical studies of the He behavior in UO_2 have shown that non-stoichiometry has an impact on He diffusion and that increasing the non-stoichiometry of the sample dramatically increases helium diffusion [10,11]. During irradiation in a nuclear reactor, UO_2 is progressively doped with fission products (FPs), more specifically with rare earths and it is expected to remain stoichiometric or slightly hypo-stoichiometric in standard fuels [12,13]. However, Spino et al. recently reported that at burn-up around 80 GWd/tM, the fuels tend to become progressively slightly hyper-stoichiometric due to the stagnation of the oxygen up-take by the cladding and in the oxidation of the fission product Mo [14]. The spent fuel is in turn a complex system with different defect structures (vacancies, interstitial oxygens, inter- and intragranular bubbles, and dislocation loops), which in turn could create local non-stoichiometric domains in the matrix. Therefore, experimental studies on the stoichiometry effect on helium solubility and diffusion have a great value, in order to shed light on this open question.

In a previous work, we have studied helium dissolution and diffusion in UO_2, UO_{2+x}, and U_3O_8 samples [15]. To have a comprehensive picture on the helium behavior in non-stoichiometric UO_2 systems, this work is aimed at studying the helium behavior in hypo-stoichiometric UO_2. Experimental studies on hypo-stoichiometric urania are complicated because this defective structure is stable only at high temperatures and samples which need to be prepared by special treatments (reducing conditions, high temperature) are then unstable at room temperature [17–21]. Baichi et al. recently reviewed the experimental results for the phase diagram data of the U–O system in U–UO_2 composition range [16]. Oxygen vacancies are presumed to be the predominant defects at $x < 0$. At temperatures below the phase transition temperature, the presence of highly energetic oxygen vacancy defects makes hypo-stoichiometric urania unstable with respect to the dissociation into metallic uranium and stoichiometric UO_2 and absorption of oxygen from atmosphere [17–21].

The yield of fission product lanthanum in the fission of uranium is relatively high, and it forms solid solutions with UO_2 over a wide range of compositions [22–25]. Doping UO_2 with a trivalent solute such as lanthanum can create an oxygen vacancy environment that is similar to the one in the hypo-stoichiometric UO_2 configuration. La^{3+} enters the host lattice as substitution on the U^{4+} sites of the cation sublattice with charge-compensation taking place by creation of vacancies on the anion sublattice.

The issue of helium generation in fuels for the transmutation of minor actinides such as $(U_{1-y}Am_y)O_{2-x}$ is an even greater issue than for conventional spent fuel. The quantities of helium produced can be a factor 10 higher than the inert gases Xe and Kr. Furthermore, $(U_{1-y}Am_y)O_{2-x}$ must be prepared in the hypo-stoichiometric regime to ensure no deleterious interaction with the cladding (oxidation

* Corresponding author at: Present address: Laboratory for Radio and Environmental Chemistry, Paul Scherrer Institut, Villigen PSI, CH-5232 Villigen, Switzerland. Tel.: +41563102407.
E-mail address: zeynep.talip@gmail.com (Z. Talip).

http://dx.doi.org/10.1016/j.nme.2015.01.002

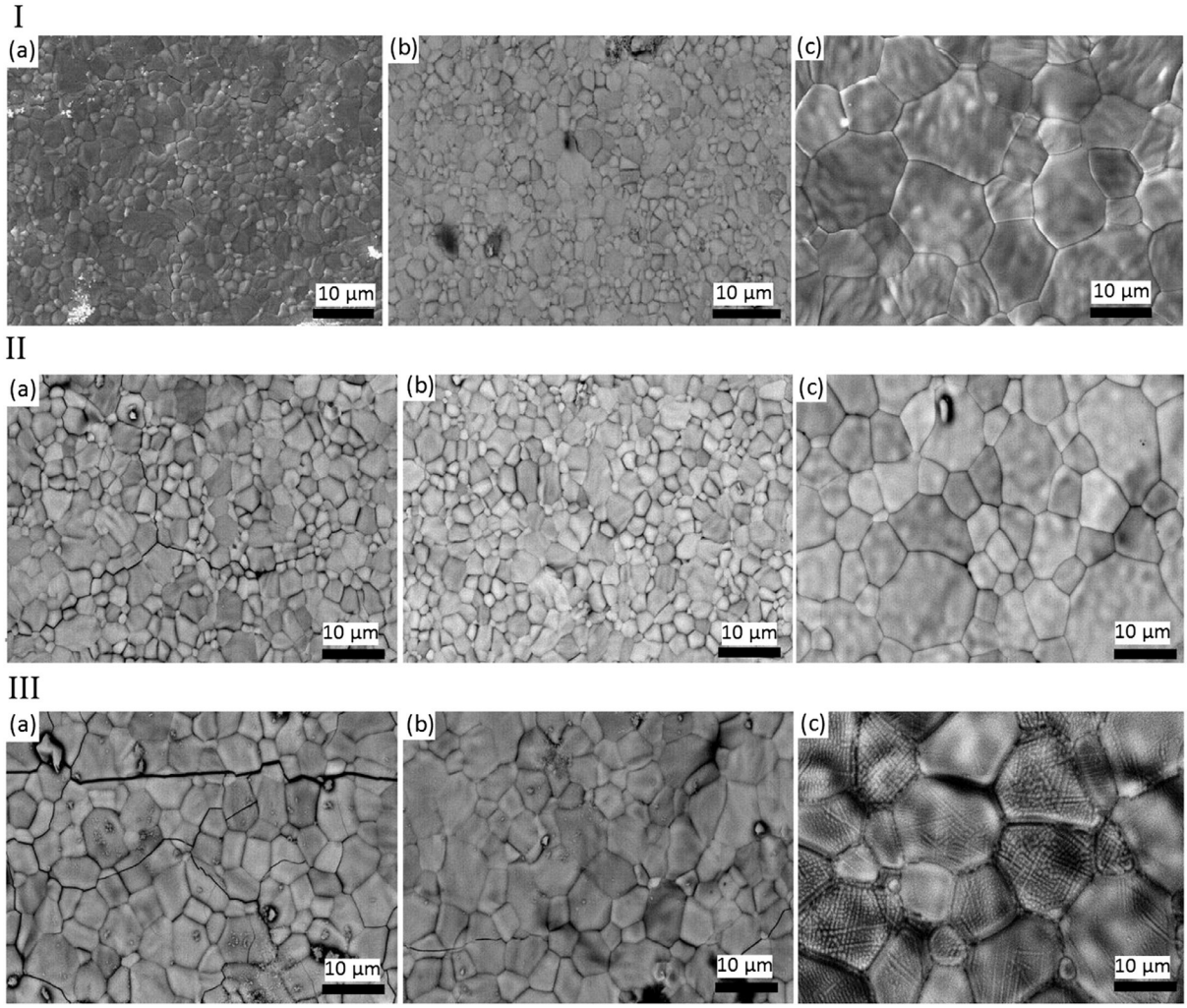

Fig. 1. SEM image of $U_{0.94}La_{0.06}O_{1.97}$ (I), $U_{0.89}La_{0.11}O_{1.95}$ (II), $U_{0.78}La_{0.22}O_{1.89}$ (III) samples before infusion (a), after infusion (b), and after thermal desorption measurements (c).

thereof). Thus La-based analogs provide an ideal source to perform dedicated separate effects studies on helium behavior in these transmutation fuels [26–29].

The aim of this study is to understand the helium behavior in hypo-stoichiometric UO_2, and the use of lanthanum, a fission product and a proxy for trivalent americium, will also help to understand the effect of cation substitution on helium dissolution on nuclear fuel. Three different UO_2 samples, containing 6, 11, and 22 mol% lanthanum, respectively, were examined. Helium was introduced in the samples by the infusion technique, and its release rate as a function of annealing temperature and quantitative measurements were performed by Laser Knudsen Cell and Quantitative Gas Measurement Systems, respectively [30,31]. Characterization of the samples was performed by scanning electron microscopy (SEM) and transmission electron microscopy (TEM).

2. Experimental

La-doped UO_2 samples with three different compositions were prepared by the sol-gel technique [32]. Powders were pressed at 110 MPa into disks that were subsequently sintered at 1923 K under reducing atmosphere (6% H_2, 94% Ar atmosphere) for 6 hours. In order to verify the formation of $U_{1-y}La_yO_{2-y/2}$ solid solutions and the presence of oxygen vacancies in the structure, X-ray diffraction (XRD) and Raman spectroscopy analyses of the samples were performed and discussed elsewhere [33]. The existence of oxygen vacancies in La-doped UO_2 samples was demonstrated by the presence of a band at ~ 540 cm^{-1} in their Raman spectra. The thickness and the weight of the samples used for the helium infusion experiments were ~0.4 mm and ~40 mg, respectively.

Microstructural characterizations of the samples were performed, using a scanning electron microscope (SEM) Vega Tescan TS5130LSH operating at 30 KeV. The average grain size (mean linear intercept) of the samples was measured with ImageJ [34] and a conversion factor considering grains have equivalent sphere diameter [35]. Concentration mapping and measurements of uranium and lanthanum and samples were performed by energy-disperse X-ray spectroscopy (OXFORD-INCA).

Transmission electron microscopy (TEM) investigations were performed with a FEI Tecnai G2 F20 XT specially modified for the analyses of radioactive materials [36]. The TEM operates at 200 kV and

Table 1
Measured grain diameter of the samples before and after thermal desorption measurements.

	Before TDS (μm)	After TDS (μm)	Final annealing temperature (K)
$(U_{0.94}La_{0.06})O_{1.97}$	3	13	2300
$(U_{0.89}La_{0.11})O_{1.95}$	4	9	2100
$(U_{0.78}La_{0.22})O_{1.89}$	7	17	2150

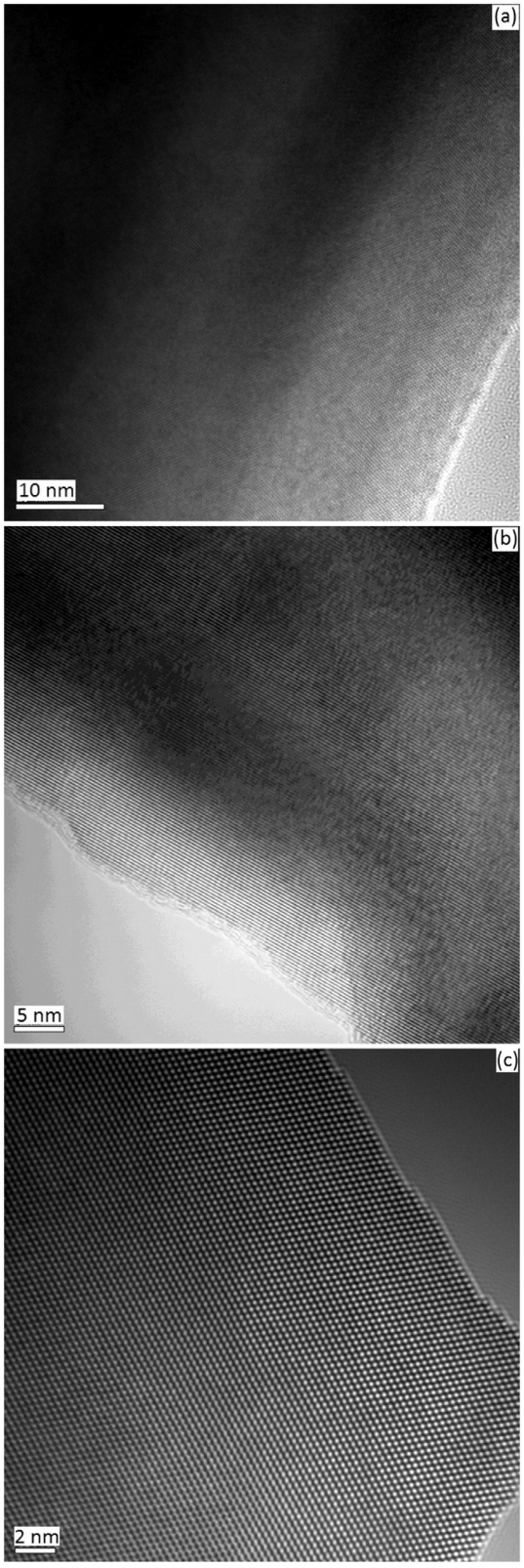

Fig. 2. Bright field TEM image of $U_{0.94}La_{0.06}O_{1.97}$ (a), $U_{0.89}La_{0.11}O_{1.95}$ (b), $U_{0.78}La_{0.22}O_{1.89}$ (c) samples.

is equipped with a Gatan GIF Tridiem camera, an additional Gatan slow scan camera, and an EDAX EDS Genesis System. The samples for the TEM observations were prepared by crushing fragments in methanol. The suspension was left for decanting, and a droplet was subsequently placed on a copper grid.

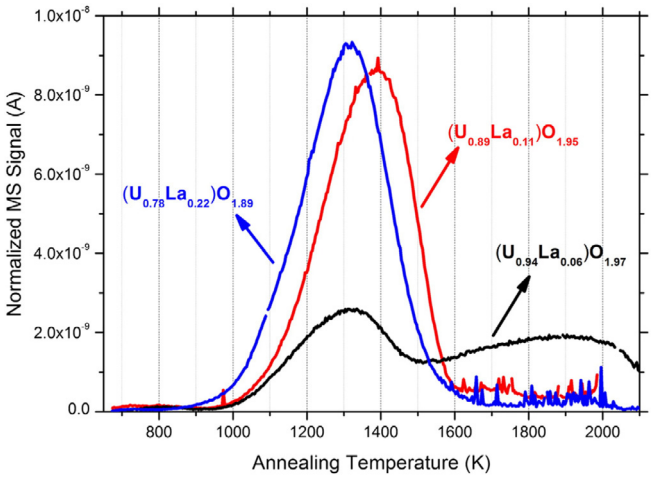

Fig. 3. Comparison of helium release rates as a function of temperature from La-doped UO_2 samples (infusion conditions: 987 atm, 1300 K, 2 hours).

The experimental configuration applied for studying helium behavior in the La-doped UO_2 materials consists of three steps. Firstly, Helium Infusion Device (HEIDI) [7] was used to incorporate helium in the different La-doped UO_2 disks by heating them with a laser (continuous wave 5 kW Nd: YAG laser at 1064 nm) at 1300 K for 120 minutes and under 987 atm helium pressure (He 6.0 impurities: O_2 < 100 ppb, H_2O < 500 ppb, CO + CO_2 < 100 ppb, THC < 100 ppb, N_2 < 100 ppb). Subsequently, the helium infused La-doped UO_2 samples were annealed in a laser-heated Knudsen cell (LKC) to desorb the helium while its release rate as a function of annealing temperature was measured by a mass spectrometer (Pfeiffer-vacuum qma 400 quadrupole mass spectrometer) and the temperature by a pyrometer, respectively. The released He gas was collected and quantitatively measured by Quantitative Gas Measurement System with its own mass spectrometer (Pfeiffer-vacuum qma 400 quadrupole mass spectrometer) by spiking a known quantity of helium gas. The details of the set-ups used can be found in ref [30,31].

3. Results and discussion

3.1. Electron microscopy observations

The microstructure of the UO_2 samples, especially their grain size, has a strong influence on helium diffusion [37]. Pore migration is expected to control the grain growth kinetics for undoped UO_2 [38]. However, it was reported that the residual pore volume has very little effect on the final grain size of Cr-doped UO_2 samples [39]. Microstructural characterization of the samples was performed to evaluate the effects of the La-content and annealing temperature on sample grain size before infusion, after infusion, and after thermal desorption measurements (Fig. 1). Note that the analysis of grain growth kinetics of La-doped UO_2 samples is out of the scope of the present study.

Table 2
Comparison of the calculated He incorporation energies for UO_2 in literature.

	Incorporation energy (eV)		
	Uranium vacancy	Oxygen vacancy	Interstitial site
Grimes, 1991[49]	−0.05	−0.12	−0.13
Crocombette et al., 2002 [46]	0.2	1.8	1.3
Petit et al., 2003 [47]	−7.4	2.2	1.3
Freyss et al., 2006 [48]	0.4	2.4	−0.1
Yakub et al., 2010 [11]	−0.02	0.3	0.45

Table 3
Theoretically calculated helium migration energies in literature.

	Energy barriers for He migration (eV)			
Initial He Position	Yakub et al. 2010 [11]	Grimes et al. 1990 [50]	Govers et al. 2009 [10]	Yun et al. 2009 [51]
OIS OIS	2.56	3.8	2.3	2.97
OIS VO OIS	0.54	0.38	0.5	0.41
OIS VU OIS	0.43	0.24	0.2	0.79

OIS: octahedral interstitial site, VO: oxygen vacancy, VU: uranium vacancy.

The SEM analyses showed that increasing the La-content in UO_2 samples results in a grain size increase from 3 to 7 μm for the 6–22 mol% La samples. While infusion (at 1300 K for 2 hours) did not have any significant impact on the grain size variation, after thermal desorption grain growth was evident (Table 1). The higher grain growth of the $(U_{0.94}La_{0.06})O_{1.97}$ sample after thermal desorption can be explained by the higher final annealing temperature (2300 K) of this sample compared to $(U_{0.89}La_{0.11})O_{1.95}$ (2100 K) and $(U_{0.78}La_{0.22})O_{1.89}$ (2150 K) samples.

Additional analyses have also been performed by TEM. TEM observations of several grains of La-doped UO_2 samples showed that all the samples have homogeneous compositions and no La or U precipitates were present in the samples (Fig. 2).

3.2. Helium thermal desorption

The main conclusion related to helium solubility in UO_2 is its low value. However, the available helium solubility data in UO_2 show a wide scattering [3–8]. In our previous study, we have observed that the dissolved helium quantity is lower in the presence of interstitial oxygen in hyper-stoichiometric UO_2 compared to stoichiometric UO_2 [15]. However, a markedly increase of the dissolved helium quantity was observed in the U_3O_8 samples which has a different crystal structure than UO_2. Comparison of the helium release as a function of temperature from the stoichiometric and hyper-stoichiometric UO_2 samples suggests that thermal helium diffusion (under vacuum) increases with increasing oxygen content of the samples. In the present study, we avoid direct comparison of the dissolved He quantities in La-doped UO_2 samples and stoichiometric UO_2 and hyper-stoichiometric UO_2 samples [15]. Hyper-stoichiometric UO_2 samples were prepared by treating of stoichiometric commercial UO_2 specimens in a suitable oxygen potential and temperature. However La-doped UO_2 samples were prepared by sol-gel technique and microstructure and density (presence of pores, intrinsic defects) of the samples which have strong impacts on He diffusion, are different than UO_2 and UO_{2+x} samples.

Fig. 3 shows the He-thermal desorption profiles (the helium release plotted as a function of temperature during a temperature ramp) of the La-doped UO_{2-x} samples as a function of temperature. The maximum of the first release peaks for the three samples were observed between 1300 and 1400 K. The two samples with the higher La-content have released most of the helium during the first step, while there is clearly a second released fraction at higher temperature for the $(U_{0.94}La_{0.06})O_{1.97}$ sample, similar to the one previously observed for pure stoichiometric UO_2 sample [15].

Table 4
Comparison of the helium diffusion coefficient and activation energies for $UO_{2\pm x}$ at 1800 K as calculated by Yakub et al. [11].

	O/U	Apparent arrhenius	Diffusion	Contribution of the vacancy
		Activation energy (eV)	Coefficient	Assisted mechanism
UO_2	1	~2.7	D	_
UO_{2+x}	2.09	~1.3	40D	35%
UO_{2-x}	1.91	<1	300D	60%

As it was shown in the previous section, grain size of the La-doped UO_2 samples increase with increasing La content. Considering grain boundaries are perfect sink for the diffusing helium, the average diffusion distance for helium to reach the grain boundaries increases with increasing grain size [37]. In contrast, faster He release was observed with increasing grain sizes of the samples. In hypo-stoichiometric UO_2, helium diffusion is considered to occur via oxygen vacancies [10] and is thus influenced by the oxygen diffusion. The oxygen diffusion coefficients for hypo-stoichiometric UO_2 were reported almost two orders of magnitude higher than those of stoichiometric UO_2 [40]. Differences between the three He-release profiles could thus be due to the acceleration of oxygen diffusion rather than grain size effect and its effect on helium diffusion when the content of dopant increases, hence when the content of oxygen vacancies is higher [33].

According to our knowledge, there are no experimental studies on helium solubility and diffusion in hypo-stoichiometric UO_2, and so far only a few experimental studies of release of fission gasses from UO_{2-x} were reported [41–43]. Felix and Miekeley reported that the diffusion coefficient for Xe is lower in UO_{2-x} and higher in UO_{2+x} samples compared to stoichiometric UO_2 [41]. Killen tried to simulate this effect by using NbO_2 and La_2O_3-doped UO_2 samples as UO_{2+x} and UO_{2-x}, respectively [42]. However, a clear relation was not obtained between doping, gas release, and irradiation behavior. Catlow predicted different trapping sites for Kr and Xe, and he considered a very fast mobility of Kr in hypo-stoichiometric oxides [43].

Experimentally, it was shown that the majority of helium atoms, if they are incorporated at low concentration in the stoichiometric UO_2 structure, occupy the interstitial octahedral sites [44]. Recently Yakub has performed a theoretical study of helium solubility in hypo-stoichiometric UO_2 by molecular dynamic (MD) simulation technique [45]. Yakub reported that the increase of the He solubility in case of hypo-stoichiometry is due to the lower He incorporation energy into an oxygen vacancy compared to the interstitial site. His conclusion is in contrast to all the previously published theoretical studies [46–48] (Table 2) but confirmed by the studies of Grimes [49]. In the present study, after infusion (under the same conditions), dissolved He quantities in $(U_{0.94}La_{0.06})O_{1.97}$, $(U_{0.89}La_{0.11})O_{1.95}$, and $(U_{0.78}La_{0.22})O_{1.89}$ samples were measured as 4.05×10^{-7}, 4.32×10^{-7}, and 5.13×10^{-7} mol g^{-1}, respectively with $\pm 2.4\%$ relative standard deviation. It should be realized that the higher La-concentration in UO_2 introduces higher concentration of oxygen vacancies in the lattice [33] which means dissolved helium quantities were slightly increased by increasing oxygen vacancy concentration in the samples. Therefore, our experimental results support the conclusion of Yakub's theoretical study.

As mentioned above, the helium diffusion mechanism in hypo-stoichiometric regions was reported as oxygen vacancy assisted and the rate-determining step of this mechanism was the jump of helium atoms between oxygen vacancies [10]. Table 3 shows the calculated migration energy of helium atoms for different paths (octahedral interstitial site, OIS, oxygen vacancy, VO, and uranium vacancy, VU) by different authors [10,11,50,51]. Energy barriers for He-migration from oxygen vacancies are much lower than interstitial sites which are considered to be a preferential migration path in stoichiometric UO_2. Both Govers and Yakub have performed theoretical studies of the helium diffusion in non-stoichiometric UO_2 [10,11]. According to their calculations, the increase of helium diffusion with deviation from stoichiometry is more pronounced in the case of hypo-stoichiometry compared to hyper-stoichiometry. The effect of non-stoichiometry on He diffusion is, however, remarkably smaller in Govers' study than in Yakub's one. Table 4 shows the comparison of the calculated helium diffusion coefficients and apparent activation energies by Yakub et al. for UO_2, $UO_{2-.09}$, and $UO_{1.91}$. As it can be seen, helium diffusion coefficient is 300 times higher in hypo-stoichiometric UO_2 than in stoichiometric UO_2. The apparent Arrhenius activation energy in

stoichiometric UO_2 is about 2.7 eV, and in hypo-stoichiometric UO_2 (O/U = 1.91), it becomes less than 1.0 eV. These values could be the explanation of the higher He release from the higher content La-doped UO_2 sample (Fig. 3).

4. Conclusions

In this study, La-doped UO_2 samples with various La-content were used to simulate hypo-stoichiometric UO_2. Comparison of the dissolved helium quantities between 6, 11, 22% mol La-doped UO_2 samples showed that the dissolved He quantities slightly increase with increasing oxygen vacancy concentration in the samples. This could be the result of the lower He incorporation energy into oxygen vacancies compared to the interstitial site as it was reported in the theoretical study of Yakub for the hypo-stoichiometric UO_2 [11]. However, even with the apparent increase of the He solubility with increasing oxygen vacancy concentration in UO_2, it should be noted that the absolute solubility remains very low and that helium precipitation can be expected for low content. In addition, it has been considered that oxygen diffusion enhances the helium diffusion in hypo-stoichiometric UO_2. However, further experiments need to be better assessed in order to quantitatively verify the oxygen diffusion effect on helium diffusion.

Acknowledgement

We would like to gratefully thank H. Hein and C. Boshoven for the sample preparation. We are further grateful to M. Ernstberger for performing numerous SEM analyses. Z. Talip also gratefully acknowledges the European Commission, Joint Research Centre, Institute for Transuranium Elements for funding her grantholder contract.

References

[1] J.-M. Gras, R.D. Quang, H. Masson, T. Lieven, C. Ferry, C. Poinssot, M. Debes, J.-M. Delbecq, J. Nucl. Mater. 362 (2007) 383–394.
[2] C. Ferry, J.-P. Piron, A. Ambard, J. Nucl. Mater. 407 (2010) 100–109.
[3] J. Belle, Proceedings of the Second United Nations International Conference on Peaceful Uses of Atomic Energy, 1958, p. 586.
[4] F. Rufeh, D.R. Olander, T.H. Pigford, Nucl. Sci. Eng. 23 (1965) 335–338.
[5] P. Sung, Equilibrium Solubility and Diffusivity of Helium in Single-Crystal Uranium Oxide, Univ, Washigton, 1967.
[6] S. Hasko, R. Szwarc, Solubility and diffusion of helium in uranium dioxide, AEC Division of Reactor Development, Washington D.C., 1963.
[7] E. Maugeri, T. Wiss, J.P. Hiernaut, K. Desai, C. Thiriet, V.V. Rondinella, J.-Y. Colle, R.J.M. Konings, J. Nucl. Mater. 385 (2009) 461–466.
[8] K. Nakajima, H. Serizawa, N. Shirasu, Y. Haga, Y. Arai, J. Nucl. Mater. 419 (2011) 272–280.
[9] G. Sattonnay, L. Vincent, F. Garrido, L. Thome, J. Nucl. Mater. 355 (2006) 131–135.
[10] K. Govers, S. Lemehov, M. Hou, M. Verwerft, J. Nucl. Mater. 395 (2009) 131–139.
[11] E. Yakub, C. Ronchi, D. Staicu, J. Nucl. Mater. 400 (2010) 189–195.
[12] Hj. Matzke, J. Nucl. Mater. 208 (1994) 18–26.
[13] Hj. Matzke, J. Nucl. Mater. 223 (1995) 1–5.
[14] J. Spino, J. Nucl. Mater. 375 (2008) 8–25.
[15] Z. Talip, T. Wiss, E.-A. Maugeri, J.-Y. Colle, P.-E. Raison, E. Gilabert, M. Ernstberger, D. Staicu, R.J.M. Konings, J. Eur. Ceram. Soc. 34 (2014) 1265–1277.
[16] M. Baichi, C. Chatillon, G. Ducros, K. Froment, J. Nucl. Mater. 349 (2006) 57–82.
[17] E. Rothwell, J. Nucl. Mater. 6 (1962) 229–236.
[18] R.G. Robins, J. Nucl. Mater. 7 (1962) 218–219.
[19] T.L. Markin, V.J. Wheeler, R.J. Bones, J. Inorg. Nucl. Chem. 30 (1968) 807–817.
[20] N.A. Javed, J. Nucl. Mater. 43 (1972) 219–224.
[21] I.I. Kapshukov, N.V. Lyalyushkin, L.V. Sudakov, A.S. Beyz, O.V. Skiba, J. Radioanal. Nucl. Chem. 143 (1990) 213–220.
[22] D.C. Hill, J. Am. Ceram. Soc. 45 (1962) 258–263.
[23] E. Stadlbauer, U. Wichmann, U. Lott, C. Keller, J. Solid State Chem. l0 (1974) 341–350.
[24] H. Kleykamp, J. Nucl. Mater. 206 (1993) 82–86.
[25] R.V. Krishnan, G. Panneerselvam, M.P. Antony, K. Nagarajan, J. Nucl. Mater. 403 (2010) 25–31.
[26] J.-F. Babelot, R. Conrad, R.J.M. Konings, G. Muhling, M. Salvatores, G. Vambenepe, J. Alloys Compd. 271-273 (1998) 606–609.
[27] E.A.C. Neeft, K. Bakker, R.P.C. Schram, R. Conrad, R.J.M. Konings, J. Nucl. Mater. 320 (2003) 106–116.
[28] A. Fernandez, J. McGinley, J. Somers, M. Walter, J. Nucl. Mater. 392 (2009) 133–138.
[29] C.T. Walker, G. Nicolaou, J. Nucl. Mater. 218 (1995) 129–138.
[30] J.Y. Colle, F. Capone, Rev. Sci. Instrum. 79 (2008) 055105.
[31] J.-Y. Colle, E.A. Maugeri, C. Thiriet, Z. Talip, F. Capone, J.-P. Hiernaut, R.J.M. Konings, T. Wiss, J. Nucl. Sci. Technol. 51 (2014) 700–711.
[32] A. Fernandez, 9th Cimtec, Innovative Materials in Advanced Energy Technologies, 1999, p. 539.
[33] Z. Talip, T. Wiss, P.E. Raison, J. Paillier, D. Manara, J. Somers, R.J.M. Konings, J. Am. Ceram. Soc. (2015), doi:10.1111/jace.13559.
[34] Rasband, W.S., ImageJ, U. S. National Institutes of Health, Bethesda, Maryland, USA, http://imagej.nih.gov/ij/, 1997-2012.
[35] P. Botazzoli, PhD Thesis, 2011, Politechnico Di Milano, Italy, 153p.
[36] T. Wiss, H. Thiele, A. Janssen, D. Papaioannou, V.V. Rondinella, R.J.M. Konings, JOM 64 (2012) 1390.
[37] Z. Talip, T. Wiss, V. Di Marcello, A. Janssen, J.-Y. Colle, P. Van Uffalen, P. Raison, R.J.M. Konings, J. Nucl. Mater. 445 (2014) 117–127.
[38] L. Bourgeois, Ph. Dehaudt, C. Lemaignan, J.P. Fredric, J. Nucl. Mater. 295 (2001) 73–82.
[39] L. Bourgeois, Ph. Dehaudt, C. Lemaignan, A. Hammou, J. Nucl. Mater. 297 (2001) 313–326.
[40] K.C. Kim, D.R. Olander, J. Nucl. Mater. 102 (1981) 192–199.
[41] F.W. Felix, W. Miekeley, J. Nucl. Mater. 42 (1972) 297.
[42] J.C. Killeen, J. Nucl. Mater. 58 (1975) 39–46.
[43] C.R.A. Catlow, Proc. R. Soc. Lond. A 364 (1978) 473–497.
[44] F. Garrido, L. Nowicki, G. Sattonnay, T. Sauvage, L. Thomé, Nucl. Instrum. Methods Phys. Res., Sect. B 219-220 (2004) 196–199.
[45] E. Yakub, J. Nucl. Mater. 414 (2011) 83–87.
[46] J.P. Crocombette, J. Nucl. Mater. 305 (2002) 29–36.
[47] T. Petit, M. Freyss, P. Garcia, P. Martin, M. Ripert, J.P. Crocombette, F. Jollet, J. Nucl. Mater. 320 (2003) 133–137.
[48] M. Freyss, N. Vergnet, T. Petit, J. Nucl. Mater. 352 (2006) 144–150.
[49] R.W. Grimes, Fundamental Aspects of Inert Gases in Solids, Plenum, New York, 1991, p. 415.
[50] R.W. Grimes, R.H. Miller, J.R.A. Catlow, J. Nucl. Mater. 172 (1990) 123–125.
[51] Y. Yun, O. Ericksson, P.M. Oppeneer, J. Nucl. Mater. 385 (2009) 510–516.